RSC Advances

PAPER

View Article Online
View Journal | View Issue

Cite this: *RSC Adv.*, 2023, **13**, 35755

A sustainable solar-driven electrochemical process for reforming lignocellulosic biomass effluent into high value-added products: green hydrogen, carboxylic and vanillic acids†

Izaías Campos da Paixão,[a] Jussara Câmara Cardozo,[a] Mayra Kerolly Sales Monteiro,[ad] Amanda Duarte Gondim,[a] Lívia Nunes Cavalcanti,[a] Domingos Fabiano de Santana Souza,[b] Carlos A. Martínez-Huitle *[ac] and Elisama Vieira dos Santos *[ac]

There is a growing concern with waste minimization and the promotion of the circular economy. Within this framework, using membrane-equipped electrochemical systems, the electrochemical oxidation (EO) of organic compounds and simultaneous hydrogen (H_2) production can considerably improve the sustainability and economic viability of this process. Here, we propose an innovative-integrate electrochemical treatment strategy to maximize the economic benefits and sustainability of selectively producing organic acids and energy-saving H_2 production from biomass platform compounds. The results clearly demonstrated that, on the one hand, more than 80 mg L^{-1} of oxalic acid was obtained in the anodic reservoir (using a boron-doped diamond electrode) with an alkaline medium (0.5 mol L^{-1} NaOH) by applying 100 mA cm^{-2} as well as vanillic acid production of 0.6795 mg L^{-1} under the same conditions. On the other hand, simultaneously green H_2 production greater than 2.6 L was produced, in the cathodic compartment with a Ni–Fe-based mesh as cathode, with a 90% faradaic efficiency during the process. Thus, the electrochemical conversion of lignocellulosic biomass effluent into high-value-added products and an energy vector was sustainably accomplished, suggesting that it is a promising energy-saving and cost-effective integrated approach for biomass valorization using solar energy.

Received 23rd August 2023
Accepted 23rd November 2023

DOI: 10.1039/d3ra05772k

rsc.li/rsc-advances

Introduction

From an economic perspective, biomass exploitation can create enormous opportunities as an emerging bioconversion tool for a circular economy due to the feasibility of these compounds to profitably convert organic matter into high value-added products and at the same time, it contributes to organic waste management.[1,2] Among the new ideas that have emerged, biomass conversion into commodity chemicals or biomass valorization are promising strategies to reduce society's dependence on fossil fuel resources.[3] These purposes filling the Nexus approach (energy, water, food, land, and climate) have a direct impact on the Sustainable Development Goals (SDGs) through integrated resource and process planning.[4]

Examining the literature related to sustainable biomass sources, several examples have demonstrated significant research into lignocellulosic biomass, promoting its conversion into sugars, fuels, carboxylic acids, and aromatic fine chemicals by electrochemical conversions.[5–9] Chemically, lignin is a phenolic polymer with a complex structure that is found in lignocellulosic biomass alongside cellulose and hemicellulose.[10] It contains with functional groups that can be used to synthesize a range of valuable functional materials, such as aromatic compounds (vanillin) and carboxylic acids by different electrochemical processes.[7–9,11,12] Concerning carboxylic acids, some of them are considered "top value-added chemicals from biomass" because they play a key role in biomass fractionation, acting as a catalyst and/or as a crucial step in polyester production.[4,13,14] In this frame, carboxylic acids are mainly produced *via* thermal processes that involve noble metal catalysts, and/or Fenton-like reactions.[15] Nevertheless, electrochemical processes for organic conversion are potentially more environmentally friendly strategies than some other processes

[a]*Renewable Energies and Environmental Sustainability Research Group, Institute of Chemistry, Federal University of Rio Grande do Norte, Campus Universitário, Av. Salgado Filho 3000, Lagoa Nova, CEP 59078-970, Natal, Rio Grande do Norte, Brazil. E-mail: carlosmh@quimica.ufrn.br; elisama.vieira@ufrn.br*

[b]*Chemical Engineering Department, Universidade Federal do Rio Grande do Norte, Senador Salgado Filho Avenue, S/N – Lagoa Nova, Natal, 59078-970, RN, Brazil*

[c]*National Institute for Alternative Technologies of Detection, Toxicological Evaluation and Removal of Micropollutants and Radioactives (INCT–DATREM), Institute of Chemistry, UNESP, P.O. Box 355, 14800 900 Araraquara, SP, Brazil*

[d]*Human Resources Program of the National Agency for Petroleum, Natural Gas and Biofuels – PRH-26-ANP, Graduate Program in Chemical Engineering – PPGEQ, Lagoa Nova, Natal, RN, 59078-970, Brazil*

† Electronic supplementary information (ESI) available. See DOI: https://doi.org/10.1039/d3ra05772k

because the electrons driving the reaction can be described as non-polluting reagents.[16,17] For these reasons, the electrochemical conversions offer the prospect of high-value-added aliphatic acid synthesis from the biomass-based platforms,[7,9] such as lignin, and it is an interesting approach that deserves attention.[18] Another factor that makes electrochemical processes preferable is that carboxylic acids are common intermediates in the EO process of various compounds, as well as being quite stable (usually oxalic, formic, acetic and maleic) and difficult to mineralize, this solution becomes even more interesting, from an environmental point of view, when wastewaters, real effluents, or more complex water matrices are used to obtain these acids.[19–21] A study by Oliveira *et al.*,[22] showed that carboxylic acids (formic, acetic and oxalic) can be obtained from the electrochemical treatment of washing machine effluents, with a particularly high level of selectivity for the production of acetic acid after 150 min of electrolysis at 60 mA cm^{-2}. The electrochemical depolymerization of lignin was also successfully carried out by using a "swiss-roll" electrochemical reactor by Wessling's group,[13] aiming to produce organic acids. Kraft lignin in 1 M NaOH as supporting electrolyte (100 mL) was pumped through the electrochemical reactor with a flow rate of 50 mL min^{-1} by applying +0.8, +2.5 and +3.5 V to combine the concepts "depollution of water and lignin depolymerization" by the formation of radicals from the water electrolysis. In fact, even when phenolic compounds, such as vanillin, are produced; the degradative-synthetic mechanism hindered its efficient conversion from lignin.

Nowadays, the trend is to design hybrid-integrated technologies that combine environmental-synthetic strategies where each part of the device performs a specific activity in a sustainable and efficient way.[23,24] At this point, there is an idea of interest that links the two goals of electrochemical systems: "*wastewater treatment and fuel generation*". In this sense, hybrid or integrated electrochemical reactors can promote the oxidation of lignin and energy-saving hydrogen production, improving the sustainability and economic viability of the process.[4,25–27] Analogous strategies have been adopted to improve this hybrid approach, using both model organic compounds with a simple structure as sacrificial analytes[28,29] and for the treatment of biodiesel[30] and glycerol[31] effluents, proving to be a good way of splitting water more efficiently, using less energy and obtaining high added value products.

Taking into account the configuration of the system, the cathode and anode compartments must be separated by a conducting membrane to prevent H_2/O_2 mixing.[32] In fact, in an anion exchange membrane system (AEM), the hydrogen evolution reaction (HER) occurs on the cathode side, while the electrooxidation of pollutants and the oxygen evolution reaction (OER) occurs on the anode side.[33,34] The H_2 produced at the cathode of the proposed electrolyzer is currently considered as a sustainable energy carrier, while the valuable low molecular weight compounds generated at the anode (electro-refinery process) can be recovered.[3,4,35,36]

Electrode selection, as anode and cathode, is the key to the success of an AEM electrolyzer.[37] On the one hand, the Ni and Fe alloys cathodic electrodes have demonstrated higher activities in alkaline media for H_2 production,[38,39] while on the other hand, among the anodic materials commonly used, boron-doped diamond (BDD) anode has outstanding ability to fragment difficult-to-degrade molecules due to the electrogeneration of oxidants such as $S_2O_8^{2-}$, $^{\bullet}OH$, chlorine species, and peroxodiphosphate.[4,40–43]

Within this framework, the aim of this work was to investigate the performance of an innovative hybrid electrochemical system using BDD and Ni–Fe as anode and cathode electrodes for the treatment of a 1 L of an effluent containing 0.5 g L^{-1} lignocellulosic biomass in NaOH as supporting electrolyte. The process was investigated by analyzing the effect of applied current density (j) and NaOH concentration (0.5, 1.0 and 2.0 mol L^{-1}) on the degradation of biomass waste with higher organic load (COD_0 = 5900 mg L^{-1}). The oxidation level of lignocellulosic biomass was also monitored using spectrophotometric analysis and COD measurements, while carboxylic acids and vanillic acid produced were monitored by high-performance liquid chromatography (HPLC) analysis. The proposed technology was driven by a photovoltaic array as an energy source to power the operation of the designed AEM-type cell, establishing a promising, efficient, and sustainable alternative to produce green H_2 and high value-added compounds as valorization approach of the lignocellulosic biomass to meet SDGs 6 and 7.

Experimental

Chemicals

Soda lignin was obtained from lignocellulosic biomass from green coconut fiber and corn cob in alkaline medium, as described in previous work by Padilha *et al.*,[44] where more information about the characterization was reported. Other chemicals, including NaOH and organic acids (oxalic, formic, and acetic acids as well as vanillic acid (standards used for the identification and quantification of organic acids)) were supplied by Sigma Aldrich and Andriol chemical (Brazil). Aqueous solutions of potassium ferri/ferro cyanide ($K_3Fe(CN)_6$/$K_4Fe(CN)_6$) ranging from 20 to 80 mmol L^{-1} in 0.5 mol L^{-1} NaOH were also prepared. Chemicals were of the highest quality commercially available and used without further purification. Anion-exchange membrane was purchased from FuMA-Tech (Fumasep FAS-50, Germany).

Electrochemical conversion system

The electrochemical treatment of lignocellulosic biomass effluent has been carried out in a homemade integrated electrochemical reactor as shown in Fig. 1a. Electrolysis experiments were performed in a two-compartment cell separated by an anion-exchange membrane (Fumasep FAS-50) at 25 °C, denominated Wastewater‖H_2 cell. Nb/BDD and Ni–Fe-based mesh were used as anode and cathode, respectively; with a working area of 16 cm^2, in both cases, and the interelectrode gap distance was kept at about 3.4 cm. Electrolysis of 1 L of 0.5 g L^{-1} lignocellulosic biomass effluent in NaOH as supporting electrolyte (which was electrolyzed at anodic compartment of

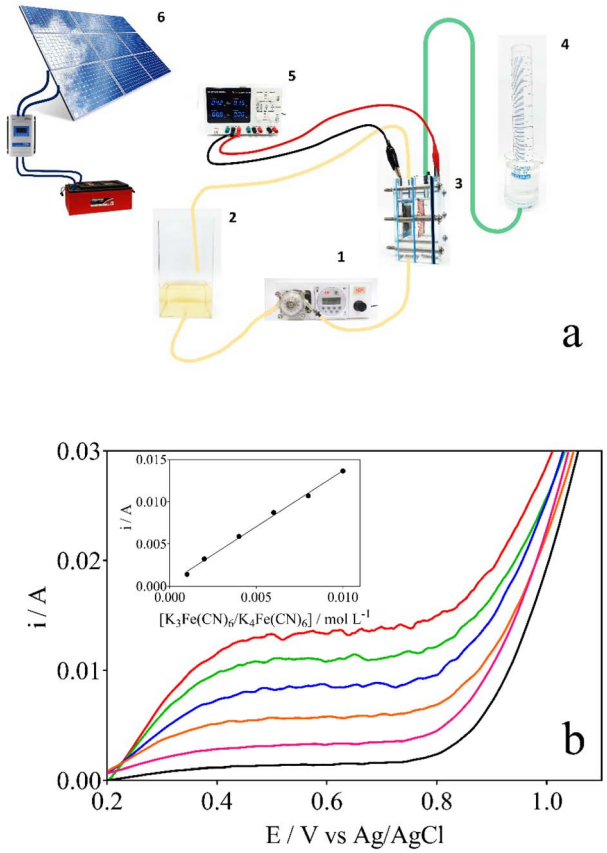

Fig. 1 (a) Schematic diagram of the complete electrochemical integrated system: (1) peristaltic pump, (2) reservoir of effluent, (3) wastewater||H_2 cell, (4) green H_2 collector, (5) power supply, (6) solar PV – battery power system. (b) Polarization curves for the k_m characterization of the electrochemical cell using ferro/ferricyanide protocol (*i.e.*, 1–10 mmol L^{-1}) in 0.5 mol L^{-1} NaOH. Inset: variations of limiting current as a function of ferro/ferricyanide concentration.

the wastewater||H_2 cell) at different concentrations (0.5, 1.0 and 2.0 mol L^{-1}) (see Table 1) were carried out during 240 min using a power supply (Minipa, model MLP-3305) under galvanostatic conditions (40, 70, and 100 mA cm^{-2}), connected to solar photovoltaic (PV)-battery system.[45] The biomass effluent was circulated through the anodic compartment by using a peristaltic pump at a constant flow rate of 125 mL min^{-1}. Meanwhile, in the cathodic compartment of the wastewater||H_2 cell, a volume of 40 mL of support electrolyte solution was used in concentrations equal to those used on the anode side, without flow conditions. At the same time, green H_2 produced was collected over distilled water at the cathodic reservoir, and the volume was measured. Before the electrolysis, the wastewater||H_2 cell characterization was performed in order to estimate the mass-transfer coefficient (k_m) and limiting current by $K_3Fe(CN)_6/K_4Fe(CN)_6$ protocol,[46] plotting polarization curves (current *vs.* potential) and using eqn (1).

$$k_m = \frac{i_L}{zFAC_\infty} \quad (1)$$

where k_m is the mass-transfer coefficient (m s^{-1}), i_L is the electrolysis limiting current (A), z is the electrons transfer in the redox reaction (for this redox pair, 1), F is the Faraday constant (96 487 C mol^{-1}), A is the electrode surface area (m^2) and C_∞ is the bulk species concentration (mol dm^{-3}). The value of the k_m was subsequently used together with the initial value of COD of the lignocellulosic biomass effluent, as required by eqn (2), to estimate the limiting current (I_{lim}), as follow:

$$I_{lim} = 4FAk_mCOD_{(t)} \quad (2)$$

where I_{lim} is the limiting current (A) at a given time t, 4 is the mean number of the electrons exchanged in the electroconversion reaction, F the Faraday constant, A the electrode area (m^2), k_m the average mass transport coefficient in the electrochemical reactor (m s^{-1}), and $COD_{(t)}$ the chemical oxygen demand (mol O_2 m^{-3}) at a given time t.

The total current efficiency (TCE) for the EO of lignocellulosic biomass effluent has been calculated, using the following relation by eqn (3):[47]

Table 1 Electrochemical conversion conditions in a wastewater||H_2 cell for the valorization of lignocellulosic biomass effluent with the production of green hydrogen as well as carboxylic and vanillic acids. The operating conditions were chosen based on the existing literature.[13,18,27]

	Experimental conditions							
				[Carboxylic acids], mg L^{-1}				
Entry	Anodic compartment	Cathodic compartment	j, mA cm^{-2}	Acetic	Formic	Oxalic	Vanillic acid, mg L^{-1}	Flow rate $r(H_2)$, mmol min^{-1}
1	0.5 mol L^{-1} NaOH + 0.5 g L^{-1} lignin	0.5 mol L^{-1} NaOH	40	13.57	14.44	70.85	0.5825 (180 min)	0.202
2	1.0 mol L^{-1} NaOH + 0.5 g L^{-1} lignin	1.0 mol L^{-1} NaOH	40	12.71	9.14	59.69	0.4810 (45 min)	0.191
3	2.0 mol L^{-1} NaOH + 0.5 g L^{-1} lignin	2.0 mol L^{-1} NaOH	40	ND[a]	15.22	55.83	0.4495 (180 min)	0.206
4	0.5 mol L^{-1} NaOH + 0.5 g L^{-1} lignin	0.5 mol L^{-1} NaOH	70	11.16	9.31	83.53	0.6505 (120 min)	0.398
5	1.0 mol L^{-1} NaOH + 0.5 g L^{-1} lignin	1.0 mol L^{-1} NaOH	70	17.11	7.75	59.96	0.5220 (60 min)	0.313
6	2.0 mol L^{-1} NaOH + 0.5 g L^{-1} lignin	2.0 mol L^{-1} NaOH	70	ND[a]	8.06	58.47	0.3530 (60 min)	0.382
7	0.5 mol L^{-1} NaOH + 0.5 g L^{-1} Lignin	0.5 mol L^{-1} NaOH	100	15.67	8.64	86.03	0.6795 (180 min)	0.504
8	1.0 mol L^{-1} NaOH + 0.5 g L^{-1} lignin	1.0 mol L^{-1} NaOH	100	8.58	9.76	86.14	0.4460 (45 min)	0.490
9	2.0 mol L^{-1} NaOH + 0.5 g L^{-1} lignin	2.0 mol L^{-1} NaOH	100	ND[a]	10.13	78.31	0.4495 (180 min)	0.502

[a] "ND" denotes "not detected".

$$\mathrm{TCE} = FV\left(\frac{\left[(\mathrm{COD})_i - (\mathrm{COD})_f\right]}{8I\Delta t}\right) \quad (3)$$

where COD (g dm^{-3}) values were considered at the initial $(COD)_i$ and final $(COD)_f$ times, respectively; I is the current (A), F the Faraday constant (96 487 C mol^{-1}), V the volume of electrolyte (dm^3) and 8 is the oxygen equivalent mass (g eq^{-1}).

Analytical techniques

The concentration of carboxylic acids (acetic, formic and oxalic) was accessed by HPLC analyses in a DIONEX system (LC Ultimate 3000) with a diode array detector (Ultimate 3000 DAD). A volume of 10 μL of sample was injected by an Ultimate 3000 autosampler. The compounds were determined by using an Acclaim Organic Acids column (Acclaim OA, 5 mm, 120 Å, 4.0 × 250 mm) at 25 °C. The mobile phase consisted of 100 mmol L^{-1} of Na_2SO_4, pH 2.65 (adjusted with methanesulfonic acid) which was eluted at 600 mL min^{-1} during 15 min. Retention times were 3.3, 4.4 and 5.6 min for oxalic, formic, acetic, respectively.[27] To reduce experimental error, each test was run twice, and the average of the replication results was used. For every determination, the differences between the series were always within 3%. The pH conditions in cathodic and anodic reservoirs were also monitored, during hybrid process, by using a HANNA pHmeter HI1131B. At the end of the same electrolysis, a Fourier transform infrared spectrometer (FTIR) was used to determine the IR spectra of untreated and treated samples to determine a modification in the internal structure of lignocellulosic biomass. For FTIR analysis, using a PerkinElmer Frontier with a sampling rate of 400–4000 cm^{-1}, the samples were deposited on the aluminum surface mirror obtained with a 3D-printed fixture lab home-made for *ex situ* measurements of specular reflectance.[48] The elimination of organic matter in the lignocellulosic biomass effluent was assessed from the changes in the COD values,[49] which was measured using pre-dosage HANNA® vials with 2 mL of sample. The samples were digested in a thermal reactor (HANNA instrument) at 150 °C for 150 min, cooled to room temperature, and analyzed using a spectrophotometer (HI83099, HANNA). Three measurements were taken, and the average value with a standard deviation of <3% was recorded.

Results and discussion

Mass transfer coefficient

Electrochemical characterization of the wastewater||H_2 cell was achieved in aqueous solutions of different concentrations of ferro/ferricyanide (*i.e.* 1–10 mmol L^{-1}) in 0.5 mol L^{-1} NaOH at a constant flow rate of 125 mL min^{-1} in the anodic compartment.[46] Fig. 1b shows that the mass transfer rate at the electrode surface is dependent on the concentration of ions in the electrolyte (a clearly defined limiting current plateau is observed), as predicted by the increase in the limiting current when an increase on the ferro/ferricyanide concentration is achieved. The plot of the obtained limiting currents as a function of the ferro/ferricyanide concentration is presented in the inset of Fig. 1b. The k_m for the wastewater||H_2 cell was estimated by eqn (1), obtaining a value about 8.58 × 10^{-5} m s^{-1}, showing that the cell design allows an effective migration of the molecules/ions towards the electrode surface during electrolysis.[46,50] Nevertheless, it is important to state that the high k_m may not necessarily

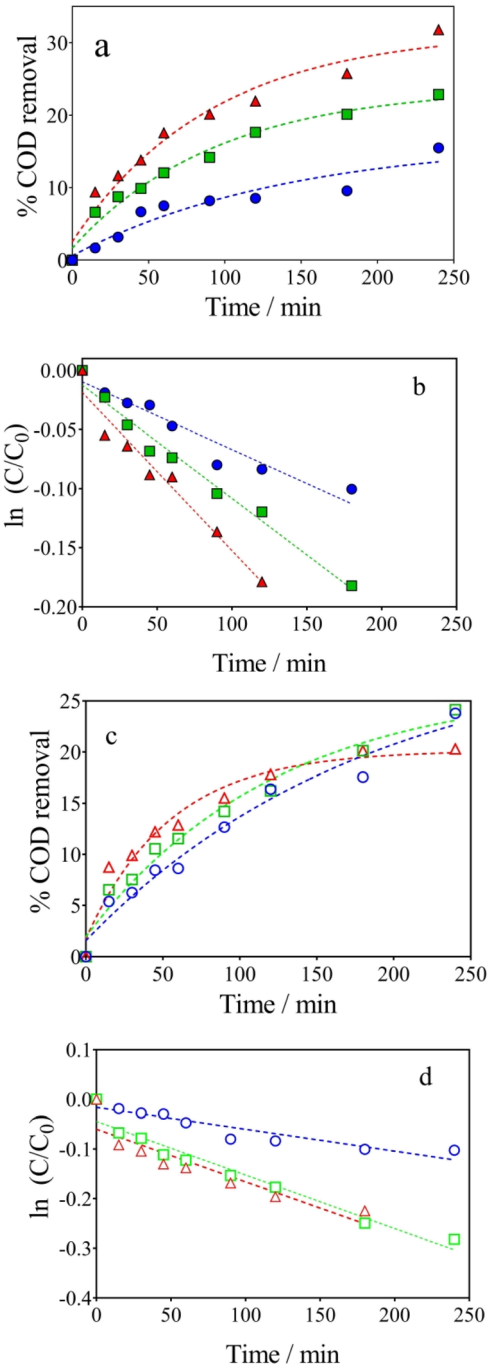

Fig. 2 (a) Effect of j, (•) 40, (■) 70 and (▲) 100 mA cm^{-2} in 2.0 mol L^{-1} NaOH, on COD removal, as a function of time; (b) kinetic analysis (pseudo-first order reaction) at different j; (c) effect of NaOH concentration, (○) 0.5, (□) 1.0 and (△) 2.0 mol L^{-1}, on the electrochemical conversion of 500 mg L^{-1} lignocellulosic biomass effluent applying 100 mA cm^{-2}; and (d) kinetic analysis at different NaOH concentration.

result in greater transformation efficiency for complex organic compounds, other operating factors, such as current density and electrolyte concentration, may influence the electrochemical conversion efficacy of the process.

Electrochemical conversion of lignocellulosic biomass

The hybrid-integrated strategy proposed here denotes an emerging concept for the production and recovery of value-added products, and energy sources where a real effluent (wastewater or complex water matrix) would only be converted into more oxidized organic species (electrochemical conversion), rather than mineralized,[51] emphasizing the concept of waste valorization or electro-refinery.[4,52,53] In order to do this, it is necessary to control the operating conditions in the wastewater$\|H_2$ cell when, for first time, the lignocellulosic biomass real effluent is electrochemically treated, especially the j and the type of supporting electrolyte, as these parameters imply the production of oxidants, such as $^{\bullet}OH$ and $S_2O_8^{2-}$, on the anode surface.[4]

In this framework, the electrochemical conversions of the lignocellulosic biomass effluent with BDD anode were investigated at different j (40–100 mA cm^{-2}) (Table 1, entries 3, 6 and 9) and electrolyte concentrations (Table 1, entries 7, 8 and 9) and are illustrated in Fig. 2a and b, respectively. For instance, 31.79% of COD removal was achieved at 100 mA cm^{-2} after 240 min of electrolysis, while 22.85% and 15.50% were accomplished by applying 70 and 40 mA cm^{-2}, respectively (Fig. 2a). Although the abilities of BDD electrodes to oxidize organic pollutants in wastewaters are well known; in this case, the efficacy of the electrochemical conversions depended on the complexity of effluent composition (being lignocellulosic biomass effluent a large and complex structure) and j.[54,55] In fact, electrochemical conversion rates (k_1), which correspond to pseudo-first order reaction, increase as a function of j, as estimated from the COD kinetic data at different j (Fig. 2b). The estimated k_1 values correspond to 0.00057 min^{-1} ($R^2 = 0.9852$), 0.00096 min^{-1} ($R^2 = 0.9801$), and 0.0014 min^{-1} ($R^2 = 0.9895$) at 40, 70, and 100 mA cm^{-2}, respectively. These results evidenced that an increase of about 2.5-folds was attained, increasing the j, but no complete mineralization was promoted.

Looking at the effect of NaOH concentration, when 500 mg L^{-1} of lignocellulosic biomass effluent were electrolyzed by applying 100 mA cm^{-2} in 0.5, 1.0 and 2 mol L^{-1} NaOH (Fig. 2c), the transformation of lignocellulose was extremely controlled,[13,18] promoting a decrease on the COD removal (from 24 to 20% when NaOH concentration was decreased). This behavior can be explained by the decrease in the amount of $^{\bullet}OH$ radicals electrogenerated at high pH, due to the increase in oxygen evolution reactions (OER),[51,56] as described by Reyter *et al.*,[57] where the OER involves the steps described in eqn (4)–(6), in alkaline solutions:

$$OH^- \rightleftarrows {}^{\bullet}OH + e^- \quad (4)$$

$$OH^- + {}^{\bullet}OH \rightleftarrows O^{\bullet} + H_2O + e^- \quad (5)$$

$$O^{\bullet} + O^{\bullet} \rightleftarrows O_2 \quad (6)$$

In this frame, the action of the $^{\bullet}OH$ radicals electrogenerated at anode surface is reduced, favoring an electrochemical conversion of the organic matter in the effluent.

In fact, it was also confirmed by COD kinetic analysis (Fig. 2d), which considers a pseudo-first-order behavior, achieving k_1 values of about 0.00044 min^{-1} ($R^2 = 0.9862$), 0.00108 min^{-1} ($R^2 = 0.9887$) and 0.00116 min^{-1} ($R^2 = 0.9839$) for 0.5, 1.0 and 2.0 mol L^{-1} of NaOH, respectively. Then, it was possible to modulate the degradation power of the electro-oxidative approach to produce high value-added products by controlling the j and supporting electrolyte concentration (it agrees with the slight increase on the k_1 values as a function of the operating conditions discussed above) and consequently, the generation of oxidants. At the same time, the oxidizing species are probably driven by mass transport because the I_{lim} estimate by eqn (2) was about 0.976 A, considering an initial COD of 590 mg L^{-1}. This I_{lim} is relatively lower compared to the current values used in this study which correspond to 1.2 A and 1.6 A for 70, and 100 mA cm^{-2}, respectively, and higher than the current applied when $j = 40$ mA cm^{-2} was used (0.64 A). When it is working below the threshold current, the pollutant's decay is conducted linearly, indicating a kinetically controlled process.[51,58]

From an environmental waste valorization point of view, the formation of high value-added products, such as carboxylic and vanillic acids in the anodic compartment of the wastewater$\|H_2$ cell, was monitored and quantified. Table 1 and Fig. 3a–c report the influence of j (40–100 mA cm^{-2}) at NaOH 0.5 mol L^{-1}, on the formation of carboxylic acids, respectively. As it can be observed in Fig. 3a and Table 1, the concentration of acetic (13.57 mg L^{-1}), formic (14.44 mg L^{-1}) and oxalic (70.85 mg L^{-1}) acids increases as a function of electrolysis-time, at 40 mA cm^{-2} and 0.5 mol L^{-1} NaOH, achieving the maximum concentration in 240 min. A slight decrease was observed on the acetic (11.16 mg L^{-1}) and formic (9.31 mg L^{-1}) acids concentrations, at 70 mA cm^{-2}, while 83.53 mg L^{-1} of oxalic acid was produced. On the other hand, the accumulation of oxalic (86.03 mg L^{-1}) was more significant at 100 mA cm^{-2}, while acetic and formic acids concentrations were similar to those obtained at 40 and 70 mA cm^{-2}, at the same concentration of NaOH (0.5 mol L^{-1}) (see Table 1). From the results obtained, it is clear that a selective conversion of the lignocellulosic biomass effluent to oxalic acid (86.14 mg L^{-1}) was reached. Also, this electrotransformations are selectively favored when the NaOH concentration was increased from 0.5 mol L^{-1} to 2 mol L^{-1} ($j = 100$ mA cm^{-2}), with no formation of acetic acid (see Fig. 3d–f), and consequently, demonstrating the improved concept of an electro-refinery in organics for the production mainly of oxalic acid. The results corroborate a study carried out by Di Marino *et al.*[13] where the concepts "depollution of water and lignin depolymerization" were combined, for first time, to produce carboxylic acids and vanillin. The authors report the formation of oxalic, malonic, succinic, malic, acetic, and formic acid were produced at concentrations of 225, 11, 5.3, 5.8, 2.2 and 8.4 mg L^{-1} at 3.5 V (applying approx. 60 mA cm^{-2}) after 240 min of electrolysis. Also, the results demonstrated the production of vanillin achieving lower yields.[13] Then, our results represent

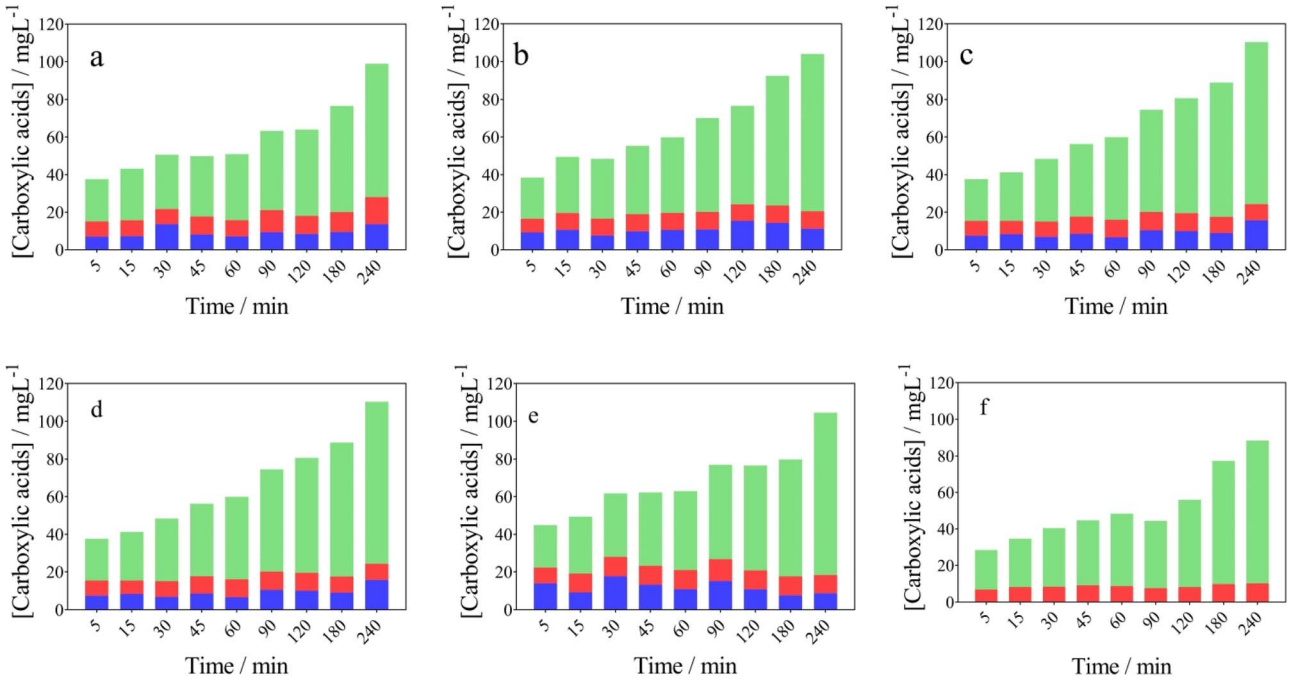

Fig. 3 Evolution of the carboxylic acids in the anodic compartment of the using the wastewater||H_2 cell: (▪) acetic, (▪) formic, and (▪) oxalic acids concentration over time. Effect of current density (a) 40, (b) 70 and (c) 100 mA cm^{-2} (Table 1, entries 1, 4 and 7) and NaOH concentration (d) 0.5, (e) 1.0, and (f) 2.0 mol L^{-1} (Table 1, entries 7, 8 and 9).

a competitive alternative to produce high value-added products from a lignocellulosic biomass effluent, as an environmental-electrosynthetic approach, with a significant selectivity. However, these could be still improved.[37]

This result also agrees with the results obtained by FTIR analysis (see Fig. S1 in the ESI†), in which, the spectra exhibit modifications during the electrochemical treatment process. The peak at 1600 cm^{-1} that corresponds to conjugated C=O, which is a characteristic of oxalic acid, increases significantly and important variations were observed in the bands related to the vibrations of the –OH that corresponds aliphatic and aromatic groups (3600 cm^{-1}).[18,59,60]

Additionally, in the lignocellulosic biomass effluent sample the peak assigned at 1120 cm^{-1} is one of the most used to identify lignin in samples,[44,61] then, the intensity of this peak is susceptible to oscillations in the concentration of this natural polymer[18,59] and it is no longer present after 120 min of EO, demonstrating that its chemical structure has been modified.

The development of an environmental-synthetic strategy using a wastewater||H_2 cell, as a selective production of di- and

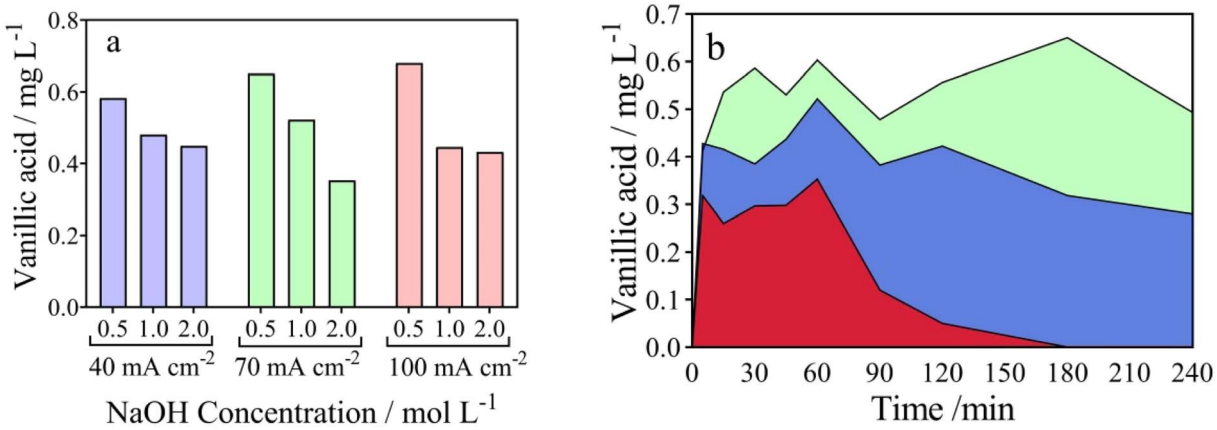

Fig. 4 The behaviour of vanillic acid production from the electrochemical treatment of 0.5 g L^{-1} of lignocellulosic biomass effluent using the wastewater||H_2 cell (a) at different electrolyte concentrations (0.5, 1.0 and 2.0 mol L^{-1} of NaOH) at the BDD electrode using 40–100 mA cm^{-2} and (b) evolution of vanillic acid as a function of time by applying 70 mA cm^{-2} in 1.0 mol L^{-1} (blue curve), 2.0 mol L^{-1} (red curve) of NaOH and 100 mA cm^{-2} in 0.5 mol L^{-1} (green curve), respectively, where the most significant concentrations were reached.

mono-carboxylic acids and energy-saving H_2 production from biomass platform compounds, has an industrial relevance. The production of organic acids is important for food, textile, tanning industries as well as the pharmaceutical manufacturing and rubber processing[4,62,63] due to their chemical properties. Then, the electro-refinery in oxalic, acetic and formic acids from lignocellulosic biomass effluent maximizes the economic benefits and the sustainability of water in agreement with the circular economy principles as an important future research topic and industrial challenge.[64,65]

It is important to indicate that, vanillic acid was also identified as a main intermediate product resulting from the EO process of lignocellulosic biomass[18,59] in the wastewater||H_2 cell, showing a peak at a retention time of 33 min (Fig. S2†). As shown in Fig. 4a, the production of vanillic acid decreases with increasing NaOH concentration, obtaining maximum concentrations (0.5825, 0.6505 and 0.6795 mg L^{-1} for j of 40, 70 and 100 mA cm^{-2} respectively) at 180 min of electrolysis. This behavior was observed at the different j studied. In the same plot, it can be seen that there is a modest increase in the production of vanillic acid when 0.5 mol L^{-1} of NaOH was used as electrolyte, as the j increases from 40 to 100 mA cm^{-2}. The influence of the NaOH concentration can also be seen in Fig. 3b where it shows that the behavior of vanillic acid generation is dependent on the electrolysis time.

Another important observation is that, among the various products of lignin oxidation, vanillin (or vanillic acid, which is an oxidized form of vanillin) is the most valuable product.[66] Vanillin offers a variety of benefits. It is an aromatic non-toxic molecule that can be chemically changed and has two reactive functionalities (the methoxy group is less reactive than the phenol and aldehyde functions).[59,66,67] Vanillin is a difunctional chemical that is beneficial in the production of thermoplastic polymers and the pharmaceutical business uses vanillin primarily as a flavoring and chemical feedstock.[59,60] Therefore, the development of suitable environmental-electrosynthetic strategies for valorizing wastewaters, using hybrid wastewater||H_2 cell approaches driven by renewable energies, constitute a substantial opportunity to produce high anodic/cathodic value-added products.

Hydrogen production

The cathodic H_2 evolution reaction (HER) under alkaline conditions was also investigated using the wastewater||H_2 cell with a Ni–Fe-based electrode in order to understand the green H_2 production capacity *via* lignocellulosic biomass effluent electro-reforming. The amount of H_2 produced was measured (Fig. 5a) and it varied linearly as a function of the electrolysis time, with a correlation factor of $R^2 > 0.995$ in all the experimental cases. This behaviour is consistent with Faraday's law.[68] Also, the electrolysis time and j directly affect the volume of H_2 produced under galvanostatic conditions (see Fig. 5a). Because the supporting electrolyte concentration in the electrolyzer's anode compartment can penetrate the anion exchange membrane into the cathode compartment, the cathodic electrode needs to exhibit stable catalytic activity for H_2 production

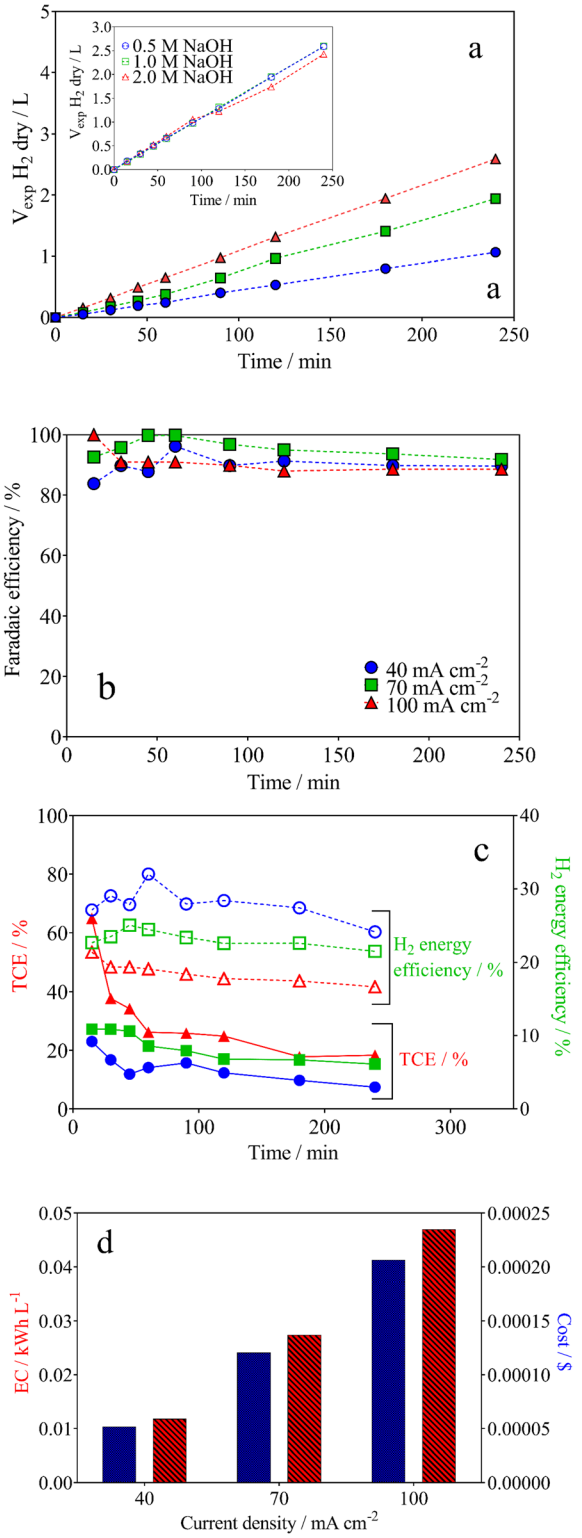

Fig. 5 (a) Volume of green H_2 produced in a hybrid process with simultaneous EO in the anodic compartment with the BDD anode, applying (•) 40, (▪) 70 and (▲) 100 mA cm^{-2} in 1 L of 500 mg L^{-1} of lignin in presence of 0.5 mol L^{-1} NaOH. Inset: influence of electrolyte concentration (b) faradaic efficiencies (in (%)) for data collected about the volume of H_2 (c) TCE estimated from the COD values measured for the electrochemical process, and energy efficiencies for electrolytic green H_2 production (d) the effect of applied current densities on the electrical energy consumption while the cost of the process was estimated based on the IRENA.

at different NaOH concentrations.[36,69] As a result, the Ni–Fe based-electrode showed efficient production of green H_2 (inset in Fig. 5a). However, it also had a partial tolerance for HER with an increase on the NaOH concentration. It provokes a decrease in the H_2 formation using 2 mol L^{-1} NaOH. This behaviour is associated to a hydrogen absorption in the metal (or at least in the surface layer), which occurs after long electrolysis times.[68,70]

From the results reported in Fig. 5a, the faradaic efficiency (FE) was estimated. As illustrated in Fig. 5b, FE fluctuated in the first 50 min of electrolysis, remaining in above 90% for the duration of the process. This behavior is due to the use of the electrical charge for anodic reactions and the existence of the fuel crossover and internal currents phenomena, in the former stage, which is a typical effect.[71]

Another important aspect that we must take into consideration is H_2 energy efficiency. This parameter in electrolysis systems can be defined as the heating value of hydrogen *versus* the rate of hydrogen produced (mol h^{-1}) divided by the energy consumed by the electrolyzer, reflecting improved thermodynamic operating conditions (eqn (7)).[72]

$$H_2 \text{ energy efficiency } (\%) = \frac{39 \text{ W h g}^{-1} \times H_2 \text{ rate} \times 2 \text{ g mol}^{-1}}{E_{cell} \times I_{cell}} \times 100 \quad (7)$$

For example, the H_2 production energy efficiencies using 0.5 mol L^{-1} of NaOH varied from 16 to 31% and depend on the *j* (Fig. 5c). This result suggests that the efficiency of the hybrid system depends on the biomass oxidation and H_2 production. Nevertheless, analyzing the data in Fig. 5c, H_2 energy efficiencies, in general, were about 29%, 23% and 19% at 40, 70 and 100 mA cm^{-2}, respectively. Meanwhile, the TCE values that correspond to the anodic oxidation process were about 23%, 30% and 65% for 40, 70 and 100 mA cm^{-2}, respectively, at the beginning of the electrolysis, and decreasing as a function of time (this behavior is because the OER, as parasite reaction,[51,71] consumes more energy than the total available for the biomass effluent oxidation reaction). Then, the behavior observed at TCE and H_2 energy efficiencies clearly shows that the energy applied in our hybrid system (wastewater||H_2 cell) is largely used for the main process, lignin electro-reforming under alkaline conditions.[7–9] Nevertheless, the effects of some of the parameters, such as cell design, electrode spacing, the use of separation membranes between compartments and even the current effects of the parasite reactions, should be additionally considered on the performance of the system.[39] As last observation, the efficiency of H_2 production relative to energy consumption decreases equivalently, and energy efficiency decreases with *j*.[73,74]

The results of this study can be compared with those reported in the literature. Santos *et al.*,[75] investigated the H_2 production which was simultaneously measured during the EO of methyl red dye and 2,4-dichlorophenoxyacetate in a double compartment cell (PEM cell with a cathode of Pt) applying 30 mA cm^{-2} at 25 °C using PbO_2, Sb-doped SnO_2 and Si/BDD anodes. Approximately 0.12, 0.08 and 0.06 L as well as 0.095, 0.082 and 0.065 L of H_2 were produced in 60 min of electrolysis from the EO of methyl red dye and 2,4-dichlorophenoxyacetate in aqueous solutions respectively for the non-active anodes, PbO_2, Si/BDD and Sb-doped SnO_2 anodes, respectively.[75] Meanwhile, the green H_2 volume produced in a hybrid process (with a Ni–Fe-based mesh as cathode) with simultaneous EO of Calcon dye[71] in the anodic compartment with the BDD anode was approximately 0.3 L by applying 30 mA cm^{-2} at 25 °C. From these results, it is possible to infer that, the production of H_2 is dependent on the surface area of the anode material, cathode nature and the electrical requirements (*i.e.*: current intensity) to promote both process in the wastewater||H_2 cell. Then, the challenge is to investigate the operating conditions to upgrading the solar-driven electrochemical hybrid process.[76]

Knowing that the Pareto graphic analysis provides pertinent data and it demonstrates the importance of the components and interactions in the system, the contributions of the effects (*j*, electrolysis time and NaOH concentration) on green H_2 production were analyzed (Fig. S3†). Obtaining as responses related to the contribution of the factors, 4.84%, 11.00% and −0.46%, for *j*, electrolysis time and supporting electrolyte concentration, respectively, indicating that the production of green H_2 is mainly affected by the electrolysis time and the intensity of the *j* to the system, while the concentration of NaOH is not a favorable factor.

Energy consumption (EC, Fig. S4†), for lignocellulosic biomass effluent electro-reforming under alkaline conditions, as a function of %COD removal, was also evaluated (inset Fig. S4†) to assess their economic viability.[77] The ratio of the specific EC, as expected, is directly proportional to the *j*. However, when %COD removal is considered, the results showed that the degradation is gradually controlled using the same electrolyte concentration, 0.5 mol L^{-1} (inset Fig. S4†). This result shows that the electrochemical conversions could be previously stopped or improved in their selectivity.

Another important information is the techno-economic analysis for the hybrid-integrated system.[71] Considering the lignin electro-reforming under alkaline conditions and the simultaneous production of green H_2, it was then estimated the electric energy and cost. Like this, the green H_2 production-cost is directly proportional to the electricity consumed (Fig. 5d). Nevertheless, the electric EC of photovoltaic system for H_2 production is obtained to according to the following equation:

$$E_s = \frac{E_{stack} \times I_{stack} \times t}{V H_2} \quad (8)$$

where E_s is the specific EC, I_{stack} is the stack current, E_{stack} is the stack voltage, VH_2 is the H_2 mass flow rate (L), and *t* (h) is the time. As can be seen in Fig. 5d, the increase of *j* produces an increase on the EC. Fig. 5d shows the EC values for different *j* of about 0.010 kW h L^{-1} H_2, 0.024 kW h L^{-1} H_2 and 0.041 kW h L^{-1} H_2 for 40, 70 and 100 mA cm^{-2}, respectively. Then, the cost related to the lignocellulosic biomass electro-reforming and H_2 production using PV system can be estimated according to the International Renewable Energy Agency (IRENA) where (1 kW h

= 0.0057$ (IRENA website[78])), which was about 0.00006, 0.00014 and 0.00024 US$ per L for H_2 produced at 40, 70 and 100 mA cm^{-2}, respectively.[79]

Conclusions

The electrochemical conversions represent a sustainable alternative for converting biomass feedstock chemicals into value-added chemicals. COD measurement suggests only a minimal loss in carbon in the system (approximately 30%), confirming the high yields. Our findings represent a crucial step for the exploitation of lignocellulosic biomass effluent for producing of valuable chemicals and fuels. High yields of carboxylic acids (oxalic = 86.03 mg L^{-1}) and vanillic acid (0.6795 mg L^{-1}) are obtained under the same experimental conditions (0.5 mol L^{-1} NaOH and J = 100 $mAcm^{-2}$) without the need for expensive catalysts or complex reactors. When coupling feedstock chemical oxidation at the anode with HER at the cathode, the hybrid electrolysis (wastewater||H_2 cell) system can also minimize impacts on the environment, and produce H_2 as a chemical energy carrier, thus favoring the circular economy. The electrochemical conversion of biomass effluent into high-valued products and energy was then successfully completed, indicating that it is a cost- and energy-efficient method for valuing biomass utilizing solar energy as well as it is a novel strategy as a potential alternative for the future supply of renewable aviation fuels in the direction of Power-to-Liquids research.

Author contributions

Izaías Campos da Paixão: methodology, investigation, validation, formal analysis. Jussara C. Cardozo: writing – original draft preparation, methodology, investigation, validation, formal analysis. Mayra Kerolly Sales Monteiro: methodology, investigation, validation, formal analysis. Domingos Fabiano de Santana Souza: conceptualization and resources. Amanda D. Gondim: resources, funding, acquisition. Livia N. Cavalcanti: resources, funding, acquisition. Elisama V. dos Santos: supervision, project administration, funding acquisition. Carlos A. Martínez-Huitle: conceptualization, supervision, writing – reviewing and editing, resources, funding acquisition.

Conflicts of interest

There are no conflicts of interest to declare.

Acknowledgements

Financial support from Conselho Nacional de Desenvolvimento Científico e Tecnológico (CNPq, Brazil) (306323/2018-4, 312595/2019-0, 439344/2018-2, 315879/2021-1, 409196/2022-3, 408110/2022-8), and from Fundação de Amparo à Pesquisa do Estado de São Paulo (Brazil), FAPESP 2014/50945-4 and 2019/13113-4, are gratefully acknowledged. Jussara C. Cardozo acknowledge the financial support under post-doctoral grants awarded by CNPq (351605/2022-3). Carlos A. Martínez-Huitle acknowledges the funding provided by the Alexander von Humboldt Foundation (Germany) and CAPES (Brazil) as a Humboldt fellowship for Experienced Researcher (88881.136108/2017-01) at the Johannes Gutenberg-Universität Mainz, Germany.

References

1 S. K. Tiwari, M. Bystrzejewski, A. De Adhikari, A. Huczko and N. Wang, *Prog. Energy Combust. Sci.*, 2022, **92**, 101023.
2 M. C. Medeiros, S. S. L. Castro, E. V. dos Santos, M. A. Rodrigo and C. A. Martínez-Huitle, *Electrochem. Commun.*, 2022, **141**, 107356.
3 M. Aziz, A. Darmawan and F. B. Juangsa, *Int. J. Hydrogen Energy*, 2021, **46**, 33756–33781.
4 E. V. dos Santos, C. A. Martínez-Huitle and M. A. Rodrigo, *Curr. Opin. Electrochem.*, 2023, **39**, 101267.
5 M. Zirbes and S. R. Waldvogel, *Curr. Opin. Green Sustainable Chem.*, 2018, **14**, 19–25.
6 O. Movil-Cabrera, A. Rodriguez-Silva, C. Arroyo-Torres and J. A. Staser, *Biomass Bioenergy*, 2016, **88**, 89–96.
7 W. Den, V. K. Sharma, M. Lee, G. Nadadur and R. S. Varma, *Front. Chem.*, 2018, **6**, 141.
8 J. Xu, Q. Zhai, F. Long, X. Jiang, S. Han and J. Jiang, *J. For. Eng.*, 2022, **7**, 11–12.
9 C. Coutanceau, N. Neha and T. Rafaïdeen, *Curr. Opin. Electrochem.*, 2023, **38**, 101210.
10 K. Malik, P. Sharma, Y. Yang, P. Zhang, L. Zhang, X. Xing, J. Yue, Z. Song, L. Nan, S. Yujun, M. M. El-Dalatony, E. S. Salama and X. Li, *Ind. Crops Prod.*, 2022, **188**, 115569.
11 T. Wang, M. Jiang, X. Yu, N. Niu and L. Chen, *Sep. Purif. Technol.*, 2022, **302**, 122116.
12 X. Ma, J. Ma, M. Li, Y. Gu and T. Wang, *Polym. Degrad. Stab.*, 2022, **204**, 110091.
13 D. Di Marino, T. Jestel, C. Marks, J. Viell, M. Blindert, S. M. A. Kriescher, A. C. Spiess and M. Wessling, *ChemElectroChem*, 2019, **6**, 1434–1442.
14 R. Gudiukaite, A. K. Nadda, A. Gricajeva, S. Shanmugam, D. D. Nguyen and S. S. Lam, *J. Environ. Manage.*, 2021, **300**, 113831.
15 L. Pola, S. Collado, P. Oulego and M. Díaz, *J. Environ. Chem. Eng.*, 2019, **7**, 103472.
16 C. A. Martínez-Huitle and M. Panizza, *Curr. Opin. Electrochem.*, 2018, **11**, 62–71.
17 S. O. Ganiyu, C. A. Martínez-Huitle and M. A. Rodrigo, *Appl. Catal., B*, 2020, **270**, 118857.
18 M. Zirbes and S. R. Waldvogel, *Curr. Opin. Green Sustainable Chem.*, 2018, **14**, 19–25.
19 S. Periyasamy and M. Muthuchamy, *J. Environ. Chem. Eng.*, 2018, **6**, 7358–7367.
20 M. C. Medeiros, E. V. dos Santos, C. A. Martínez-Huitle, A. S. Fajardo and S. S. L. Castro, *Sep. Purif. Technol.*, 2020, **250**, 117099.
21 D. Villaseñor-Basulto, A. Picos-Benítez, N. Bravo-Yumi, T. Perez-Segura, E. R. Bandala and J. M. Peralta-Hernández, *J. Electroanal. Chem.*, 2021, **895**, 1–7.
22 H. L. Oliveira, T. M. Barros, J. E. L. Santos, A. D. Gondim, M. A. Quiroz, C. A. Martínez-Huitle and E. V. dos Santos, *Electrochem. Commun.*, 2023, **154**, 107553.

23 C. A. Martínez-Huitle, I. Sirés and M. A. Rodrigo, *Curr. Opin. Electrochem.*, 2021, **30**, 100905.
24 J. W. Lee, B. Kim, J. Y. Seo, Y. S. Kim, P. J. Yoo and C.-H. Chung, *Appl. Surf. Sci.*, 2023, **610**, 155524.
25 C. Z. Smith, J. H. P. Utley and J. K. Hammond, *J. Appl. Electrochem.*, 2011, **41**, 363–375.
26 L. Handojo, A. K. Wardani, D. Regina, C. Bella, M. T. A. P. Kresnowati and I. G. Wenten, *RSC Adv.*, 2019, **9**, 7854–7869.
27 M. C. Medeiros, S. S. L. Castro, E. V. dos Santos, M. A. Rodrigo and C. A. Martínez-Huitle, *Electrochem. Commun.*, 2022, **141**, 107356.
28 B. Guenot, M. Cretin and C. Lamy, *J. Appl. Electrochem.*, 2015, **45**, 973–981.
29 C. Lamy, A. Devadas, M. Simoes and C. Coutanceau, *Electrochim. Acta*, 2012, **60**, 112–120.
30 N. Chuenangkul, K. Serivalsatit, M. Hunsom and K. Pruksathorn, *J. Water Process Eng.*, 2022, **46**, 101989.
31 A. T. Marshall and R. G. Haverkamp, *Int. J. Hydrogen Energy*, 2008, **33**, 4649–4654.
32 L. Du, Y. Sun and B. You, *Mater. Rep.: Energy*, 2021, **1**, 100004.
33 T. Pandiarajan, L. J. Berchmans and S. Ravichandran, *RSC Adv.*, 2015, **5**, 34100–34108.
34 I. Vincent, E. C. Lee and H. M. Kim, *RSC Adv.*, 2020, **10**, 37429–37438.
35 J. Nowotny, C. C. Sorrell, L. R. Sheppard and T. Bak, *Int. J. Hydrogen Energy*, 2005, **30**, 521–544.
36 M. Ball, W. Weindorf and U. Bünger, in *The Hydrogen Economy*, ed. M. Ball and M. Wietschel, Cambridge University Press, Cambridge, 2009, pp. 277–308.
37 I. Vincent and D. Bessarabov, *Renewable Sustainable Energy Rev.*, 2018, **81**, 1690–1704.
38 L. Zeng, T. Yuan, Z. Liu, Y. Zhu, D. Wu, D. Wang, Q. Zhou and R. Tang, *J. Colloid Interface Sci.*, 2023, **634**, 897–905.
39 J. E. L. Santos, D. R. Da Silva, C. A. Martínez-Huitle, E. V. Dos Santos and M. A. Quiroz, *RSC Adv.*, 2020, **10**, 37695–37706.
40 Í. L. de Oliveira, A. L. O. da Silva, M. C. Medeiros, K. F. Magalhães, C. C. O. Morais, C. A. Martínez-Huitle and S. S. L. Castro, *J. Electroanal. Chem.*, 2022, **911**, 116224.
41 S. O. Ganiyu, C. A. Martínez-Huitle and M. A. Oturan, *Curr. Opin. Electrochem.*, 2021, **27**, 100678.
42 K. C. Freitas de Araújo, K. N. de Oliveira Silva, M. K. Monteiro, D. Ribeiro Da Silva, E. V. dos Santos, M. A. Quiroz and C. A. Martínez-Huitle, *J. Electrochem. Soc.*, 2022, 2–11.
43 M. K. Sales Monteiro, M. M. Sales Monteiro, A. M. de Melo Henrique, J. Llanos, C. Saez, E. V. Dos Santos and M. A. Rodrigo, *Curr. Opin. Electrochem.*, 2021, 100685.
44 C. E. de A. Padilha, C. da C. Nogueira, S. C. B. Matias, J. D. B. da Costa Filho, D. F. de S. Souza, J. A. de Oliveira and E. S. dos Santos, *Colloids Surf., A*, 2020, **603**, 125260.
45 J. M. M. Henrique, M. K. S. Monteiro, J. C. Cardozo, C. A. Martínez-Huitle, D. R. da Silva and E. V. dos Santos, *J. Electroanal. Chem.*, 2020, **876**, 114734.
46 M. A. Quiroz, U. A. Martínez-Huitle and C. A. Martínez-Huitle, *J. Mex. Chem. Soc.*, 2005, **49**, 279–283.
47 C. A. Martínez-Huitle, C. C. de Almeida, A. S. Fajardo, S. Ferro and A. De Battisti, *J. Electrochem. Soc.*, 2017, **164**, E375–E378.
48 J. H. da Silva Junior, J. V. de Melo and P. S. Castro, *Microchim. Acta*, 2021, **188**, 1–9.
49 C. M. de Castro, P. Olivi, K. C. de Freitas Araújo, I. D. Barbosa Segundo, E. V. dos Santos and C. A. Martínez-Huitle, *Sci. Total Environ.*, 2023, **855**, 158816.
50 C. A. Martínez-Huitle, S. Ferro and A. De Battisti, *J. Appl. Electrochem.*, 2005, **35**, 1087–1093.
51 C. A. Martínez-Huitle, M. A. Rodrigo, I. Sirés and O. Scialdone, *Appl. Catal., B*, 2023, **328**, 122430.
52 B. Bakan, N. Bernet, T. Bouchez, R. Boutrou, J. M. Choubert, P. Dabert, C. Duquennoi, V. Ferraro, D. García-Bernet, S. Gillot, J. Mery, C. Rémond, J. P. Steyer, E. Trably and A. Tremier, *Waste Biomass Valorization*, 2022, **13**, 1267–1276.
53 X. Wang, C. Li, C. H. Lam, K. Subramanian, Z. H. Qin, J. H. Mou, M. Jin, S. S. Chopra, V. Singh, Y. S. Ok, J. Yan, H. Y. Li and C. S. K. Lin, *J. Hazard. Mater.*, 2022, **423**, 127023.
54 A. Miśkiewicz and S. Velizarov, *Sep. Purif. Technol.*, 2011, **83**, 166–172.
55 J. C. Cardozo, D. R. da Silva, C. A. Martínez-Huitle, M. A. Quiroz and E. V. dos Santos, *Electrochim. Acta*, 2022, **411**, 140063.
56 J. Niu, Y. Bao, Y. Li and Z. Chai, *Chemosphere*, 2013, **92**, 1571–1577.
57 D. Reyter, D. Bélanger and L. Roué, *Water Res.*, 2010, **44**, 1918–1926.
58 M. Panizza and G. Cerisola, *Electrochim. Acta*, 2005, **51**, 191–199.
59 P. Parpot, A. P. Bettencourt, A. M. Carvalho and E. M. Belgsir, *J. Appl. Electrochem.*, 2000, **30**, 727–731.
60 S. Gillet, M. Aguedo, L. Petitjean, A. R. C. Morais, A. M. Da Costa Lopes, R. M. Łukasik and P. T. Anastas, *Green Chem.*, 2017, **19**, 4200–4233.
61 J. Reyes-Rivera and T. Terrazas, *Methods Mol. Biol.*, 2017, **1544**, 193–299.
62 R. D. Di Lorenzo, I. Serra, D. Porro and P. Branduardi, *Catalysts*, 2022, **12**, 234.
63 R. Gudiukaite, A. K. Nadda, A. Gricajeva, S. Shanmugam, D. D. Nguyen and S. S. Lam, *J. Environ. Manage.*, 2021, **300**, 113831.
64 B. K. Mishra, S. Chakraborty, P. Kumar and C. Saraswat, *Sustainable Solutions for Urban Water Security*, Springer Nature Switzerland AG 2020, DOI: **10.1007/978-3-030-53110-2**.
65 B. Bakan, N. Bernet, T. Bouchez, R. Boutrou, J. M. Choubert, P. Dabert, C. Duquennoi, V. Ferraro, D. García-Bernet, S. Gillot, J. Mery, C. Rémond, J. P. Steyer, E. Trably and A. Tremier, *Waste Biomass Valorization*, 2022, **13**, 1267–1276.
66 M. Nasrollahzadeh, Z. Nezafat and N. Shafiei, *Biopolymer-Based Metal Nanoparticle Chemistry for Sustainable Applications: Volume 1: Classification, Properties and Synthesis*, 2021, pp. 145–183.
67 M. Garedew, C. H. Lam, L. Petitjean, S. Huang, B. Song, F. Lin, J. E. Jackson, C. M. Saffron and P. T. Anastas, *Green Chem.*, 2021, **23**, 2868–2899.

68 M. A. Quiroz, F. Córdova, E. Lamy-Pitara and J. Barbier, *Electrochim. Acta*, 2000, **45**, 4291–4298.
69 S. A. Grigoriev, V. I. Porembsky and V. N. Fateev, *Int. J. Hydrogen Energy*, 2006, **31**, 171–175.
70 B. Guenot, M. Cretin and C. Lamy, *J. Appl. Electrochem.*, 2015, **45**, 973–981.
71 J. C. Cardozo, D. R. Silva, C. A. Martínez-Huitle, M. A. Quiroz and E. V. Dos Santos, *Materials*, 2022, **15**, 7445.
72 H. Park, C. D. Vecitis and M. R. Hoffmann, *J. Phys. Chem. C*, 2009, **113**, 7935–7945.
73 M. Ni, M. K. H. Leung and D. Y. C. Leung, *Energy Convers. Manage.*, 2008, **49**, 2748–2756.
74 N. A. Burton, R. V. Padilla, A. Rose and H. Habibullah, *Renewable Sustainable Energy Rev.*, 2021, **135**, 110255.
75 J. E. L. Santos, D. R. Da Silva, C. A. Martínez-Huitle, E. V. Dos Santos and M. A. Quiroz, *RSC Adv.*, 2020, **10**, 37947–37955.
76 T. Wang, X. Cao and L. Jiao, *Angew. Chem., Int. Ed.*, 2022, **61**, e202213328.
77 J. R. Domínguez, T. González and S. Correia, *J. Environ. Manage.*, 2021, **298**, 113538.
78 IRENA, *Global Renewables Outlook: Energy Transformation 2050*, IRENA, 2020.
79 H. Nami, O. B. Rizvandi, C. Chatzichristodoulou, P. V. Hendriksen and H. L. Frandsen, *Energy Convers. Manage.*, 2022, **269**, 116162.